INFECTION AND IMMUNITY, Aug. 2004, p. 4589–4602 Vol. 72, No. 8
0019-9567/04/$08.00+0 DOI: 10.1128/IAI.72.8.4589–4602.2004

The Plague Virulence Protein YopM Targets the Innate Immune Response by Causing a Global Depletion of NK Cells

Edward J. Kerschen, Donald A. Cohen, Alan M. Kaplan, and Susan C. Straley*

Department of Microbiology, Immunology, and Molecular Genetics, University of Kentucky, Lexington, Kentucky 40536-0298

Received 5 February 2004/Returned for modification 9 March 2004/Accepted 11 May 2004

***Yersinia pestis*, the etiologic agent of plague, delivers six *Yersinia* outer proteins (Yops) into host cells upon direct bacterial contact. One of these, YopM, is necessary for virulence in a mouse model of septicemic plague, but its pathogenic function is unknown. We report here the immune processes affected by YopM during infection. To test whether the innate or adaptive immune system is targeted by YopM, C57BL/6 (B6) and B6 SCID mice were infected with either the conditionally virulent *Y. pestis* KIM5 or a *yopM* deletion mutant and evaluated for bacterial growth in spleen and liver. Both B6 and SCID mice succumbed to infection with *Y. pestis* KIM5, whereas both mouse strains survived infection by the YopM$^-$ mutant. These data showed that YopM counteracts innate defenses present in SCID mice. The YopM$^-$ strain grew more slowly than the parent *Y. pestis* during the first 4 days of infection in both mouse strains, indicating an early pathogenic role for YopM. In B6 mice, populations of cells of the immune system were not differentially affected by the two *Y. pestis* strains, with one major exception: the parent *Y. pestis* KIM5 but not the YopM$^-$ mutant caused a significant global decrease in NK cell numbers (blood, spleen, and liver), beginning early in infection. NK cells and macrophages isolated early (day 2) from livers and spleens of mice infected with either *Y. pestis* strain contained comparable levels of cytokine mRNA: interleukin (IL)-1β, IL-12, IL-15, IL-18, and tumor necrosis factor alpha in macrophages and gamma interferon in NK cells. However, by day 4 postinfection, cells from mice infected with the parent *Y. pestis* expressed lower levels of these messages, while those from mice infected with the mutant retained strong expression. Significantly, mRNA for the IL-15 receptor α chain was not expressed in NK cells from *Y. pestis* KIM5-infected mice as early as day 2 postinfection. These findings suggest that YopM interferes with innate immunity by causing depletion of NK cells, possibly by affecting the expression of IL-15 receptor α and IL-15.**

The causative agent of plague, *Yersinia pestis*, and two enteropathogenic yersiniae, *Y. enterocolitica* and *Y. pseudotuberculosis*, possess a common 70-kb plasmid that carries genes encoding secreted virulence proteins (Yops and LcrV) and regulatory proteins involved in virulence protein expression and secretion (3, 42). Upon contact with eukaryotic cells, yersiniae release LcrV into the medium and deliver six effector Yops directly into the eukaryotic cell cytoplasm through a type III secretion system. LcrV and all six effector Yops have been shown to be indispensable for virulence (4, 7, 14, 21, 25, 27, 29, 34, 40). LcrV is multifunctional: within the bacteria, it is regulatory and necessary for full activation of the type III secretion system (23, 24). It is essential for the delivery of Yops and is believed to participate in forming the channel through which the Yops pass through the host cell plasma membrane (10, 16, 24, 28). The released LcrV has been shown to cause interleukin (IL)-10 expression by monocyte/macrophages, with consequent delayed production of tumor necrosis factor alpha (TNF-α) and gamma interferon (IFN-γ) during infection (20, 21, 22, 37).

Five of the effector Yops, YopE, YopH, YopT, YpkA, and YopJ, have known cellular targets or enzymatic mechanisms and function to undermine innate defenses. YopE, YopH, YopT, and YpkA act synergistically to inhibit mobilization of the cytoskeleton and hence are antiphagocytic (4). YopE is a GPTase-activating protein for Rho family GTPases, with resulting depolymerization of actin microfilaments as well as other consequences of inactivation of Rho family GTPases (4). YopH is a protein tyrosine phosphatase that dephosphorylates proteins necessary for assembly of focal complexes and inhibits calcium signaling in neutrophils (4). YopT is a cysteine protease that inactivates RhoA, Rac-1, and Cdc42 by cleaving them from the membrane (4, 36). YpkA is a RhoA- and Rac-1-binding serine/threonine kinase (4). YopJ blocks mitogen-activated protein kinase and NF-κB signaling pathways, inhibiting the production of certain inflammatory cytokines and inducing apoptosis in macrophages through caspase activation (4).

YopM is the one Yop for which a function has not been identified. This Yop is a 46.2-kDa acidic protein that belongs to the leucine-rich repeat family of proteins and consists almost entirely of leucine-rich repeats that stack together into a horseshoe-shaped structure (4). In earlier studies it was shown that YopM binds to human α-thrombin and inhibits thrombin-induced platelet aggregation (14, 33). Later, Skrzypek et al. (38) showed that YopM initially localized in the cytoplasm and subsequently moved into the nucleus by a mechanism dependent on vesicular trafficking. YopM has been shown to form a complex with the serine/threonine kinases PRK2 and RSK1

* Corresponding author. Mailing address: Department of Microbiology, Immunology, and Molecular Genetics, University of Kentucky, Lexington, KY 40536-0298. Phone: (859) 323-6538. Fax: (859) 257-8994. E-mail: scstra01@uky.edu.

TABLE 1. List of bacterial strains used for infections

Y. pestis strain	Relevant property(ies)	LD_{50} in B6 mice (CFU)
KIM5	Parent strain, conditionally virulent	$<5.0 \times 10^1$
KIM5-3002	YopM$^-$	5.0×10^6
KIM5-3003	YopH$^-$	$>1.7 \times 10^7$

(17). Functional studies have shown that these kinases are involved in a number of cellular pathways; however, it is unknown if this complex forms in *Yersinia*-infected tissue or what role it may play in host responses during the course of infection.

In this study, we compared host responses to a conditionally virulent *Y. pestis* strain and an isogenic YopM$^-$ mutant to identify components of the immune response that are affected by YopM. Studies with C57BL/6 (B6) and B6 SCID mice revealed that, starting early after infection, YopM is necessary for virulence of the yersiniae in the absence of B and T cells; however, the adaptive immune response is required to clear the bacteria effectively. A striking global depletion of NK cells in response to the parent *Y. pestis* was the only significantly different cellular response in mice infected with the two *Yersinia* strains. This correlated with reduced levels of mRNA for IL-1β, IL-12, IL-15, IL-18, and TNF-α in macrophages and for IFN-γ in the NK cells that were present, in contrast to strong expression in cells from mice infected with the YopM$^-$ mutant. Further, mRNA for the IL-15 receptor α chain was reduced in amount as early as day 2 only in NK cells from mice infected with *Y. pestis* KIM5. Thus, we hypothesize that YopM's contribution to the lethality of plague occurs through interference with cytokine circuitry essential for maintenance and activation of NK cells, activation of macrophages, and the development of Th1 immunity.

MATERIALS AND METHODS

Bacterial strains. *Y. pestis* strains all lacked the pigmentation virulence determinant (Δ*pgm*) and hence were conditionally virulent (44) and exempt from federal select agent regulations. The parent strain used in this study, *Y. pestis* KIM5 (Table 1), was obtained from Robert R. Brubaker, Michigan State University (strain KIM10 in his nomenclature). To create the YopM$^-$ *Y. pestis* strain KIM5-3002 used in this study, the entire *yopM* gene, from −2 bp before the initiating Met codon through the stop codon, was deleted by an allelic exchange method described previously (47). The sequences flanking the deletion in the allelic exchange plasmid were created by PCR with primers given in Table 2 and cloned into the suicide vector pLD55 (18). The resulting *yopM* deletion was confirmed by PCR, DNA sequencing, and demonstrating the absence of YopM expression by the bacteria. The *yopH* deletion in *Y. pestis* KIM5-3003 was made in *Y. pestis* KIM5 with the same allelic exchange plasmid previously described for use in *Y. pestis* KIM8 (47).

Infection of mice and virulence testing. Female B6 mice (National Cancer Institute or Jackson Laboratory, Indianapolis, Ind.) or B6 SCID mice (Jackson Laboratory), 6 to 8 weeks old, were anesthetized with an isoflurane-oxygen mixture with a rodent anesthesia machine. *Y. pestis* was grown in exponential phase for ca. six generations in heart infusion broth (Difco Laboratories, Detroit, Mich.) at 26°C to A_{620} = 0.8 to 1.2. Cells were sedimented by centrifugation, washed once in phosphate-buffered saline (PBS), resuspended, and diluted in PBS. Before use, samples from the dilutions were plated on tryptose blood agar (Difco) and incubated at 30°C for later CFU determinations. Bacteria were injected intravenously via the retro-orbital plexus with 0.1 ml of bacterial suspensions. For determinations of the 50% lethal dose (LD_{50}), four mice were used per dose. Each dosage group was caged separately and observed daily for 14 days. When an LD_{50} could be calculated, the Reed and Muench method was used (32).

Determination of infection time course. A dose of 10^2 was used for monitoring bacterial growth and host response during the course of infection. Groups of three mice per time point were euthanized by hypercarbia followed by cervical luxation, and their spleens and livers were each weighed, transferred to a sterile bag containing 1 ml of PBS, and placed on ice. The tissues were homogenized in a Stomacher 80 lab blender (Tekmar Co., Cincinnati, Ohio) for 120 s. The suspensions of livers and spleens were diluted in PBS and plated in triplicate onto tryptose blood agar plates to determine viable numbers.

Histopathology. Portions of livers and spleens were placed in 10% neutralized formalin and processed through graded alcohol and xylene, followed by embedment in paraffin. Sections stained with hematoxylin and eosin were examined and photographed with an Axiophot microscope (Carl Zeiss, Inc., Batavia, Ill.) and Spot digital camera (Diagnostic Instruments, Inc., Sterling Heights, Mich.).

Flow cytometry. Cells isolated from the liver, spleen, and blood were analyzed in a FACSCalibur flow cytometer (Becton-Dickson FACS Systems, Mountain View, Calif.). Briefly, samples of liver and spleen were placed in sterile bags containing 10 ml of RPMI 1640 (Life Technologies Inc., Grand Island, N.Y.). The tissue was processed with the Stomacher 80 lab blender. The homogenized tissue was centrifuged and resuspended in 2 ml of 150 mM NH_4Cl, pH 7.0, to lyse red blood cells. After 2 min, the reaction was stopped by addition of 10 ml of PBS containing 1% (wt/vol) bovine serum albumin (BSA) and 0.1% (wt/vol) sodium azide (PBS-BSA-azide). Nonlysed cells were centrifuged and resuspended in PBS-BSA-azide. The resulting samples all had similar total numbers of cells. The cells were filtered through a 70-μm-pore-size nylon filter, and portions of the cells were stained with antibody-fluorochrome conjugates. For cells from blood, 0.5 ml of blood was collected by heart puncture from euthanized mice and mixed with 0.1 ml of heparin (1,000 μ/ml) on ice. The blood was then mixed with 1 ml of PBS, layered onto 1 ml of Lympholyte-Mammal (Cedarlane Labs), and centrifuged at 800 × *g* for 20 min. Nonpelleted leukocytes were washed twice in PBS-BSA-azide and finally resuspended in 0.1 ml of the same buffer.

The following antibodies were purchased from BD Pharmingen, Inc. (San Diego, Calif.) and used for the flow cytometric analysis: allophycocyanin-conjugated anti-CD45 for all hematopoietic cells, fluorescein isothiocyanate-conjugated anti-CD4 and phycoerythrin-conjugated anti-CD8 for T cells, indodicarbocyanine-conjugated anti-F4/80 for macrophages, fluorescein isothiocyanate-conjugated anti-CD19 for B cells, phycoerythrin-conjugated anti-NK1.1 and fluorescein isothiocyanate-conjugated anti-CD49b for NK cells, and phycoerythrin-conjugated anti-Gr1 for neutrophils. Cells were incubated on ice for 1 h in the presence of the appropriate antibodies, washed in PBS, and finally resuspended in ice-cold PBS containing 4% (wt/vol) paraformaldehyde, pH 7.4.

Prior to analysis, the cells were counted, and samples were adjusted to have the same cell number (2.5×10^7 cells). All samples were initially gated on CD45 to identify hematopoietic cells. To analyze lymphocyte populations (T-cell subsets and B cells), CD45$^+$ cells were gated by forward and side scatter, and then the total numbers of lymphocyte-sized cells that expressed the indicated surface marker were determined. Similarly, a gate based on forward and side scatter was set for the expected size of myeloid cells (monocytes/macrophages and granulocytes) prior to analysis of fluorescent markers. At least 20,000 gated events were acquired for each analysis. No additional gating was used on CD45$^+$ cells for analysis of NK cells.

Magnetic bead sorting and mRNA analysis. Samples of liver and spleen were processed as described for flow cytometric analysis except that tissue samples from the three mice per datum point were pooled. For magnetic bead capture, 10^8 cells were stained with either phycoerythrin-anti-NK1.1 for NK cell purification or indodicarbocyanine-anti-F4/80 for macrophage purification. Cells were stained for 1 h on ice, washed in PBS, and then mixed with either phycoerythrin- or indodicarbocyanine-specific MACS magnetic beads (Miltenyi Biotec, Auburn, Calif.). Cell-bead complexes were separated on magnetic columns as recommended by the manufacturer. Eluted cells were evaluated for purity by flow cytometry. In general, macrophages were ca. 88% pure, and NK cells were ca. 96% pure. mRNA was isolated from purified cells and from unfractionated samples of liver and spleen with Trizol (Invitrogen Corp., Carlsbad, Calif.) according to the manufacturer's protocol, and the concentrations of purified RNA were determined by spectrophotometry.

Purified RNA was reverse transcribed with a reverse transcription kit (Promega, Madison, Wis.) to generate cDNA, followed by PCR in a Perkin-Elmer thermocycler. The expression of IFN-γ, IL-15, IL-15Rα, and β-actin (Table 2) was examined in NK cells, while that for IL-1, IL-4, IL-6, IL-10, IL-12 p40 (regulated subunit), IL-15, IL-15Rα, IL-18, TNF-α, and β-actin (Table 2) was examined in macrophages. All PCRs were run under the conditions of 1 min at 95°C, 1 min at 55°C, and 1 min at 72°C for 35 cycles, except for β-actin, which was run for 25 cycles. Positive control samples for IL-10 and IL-4 were prepared from mouse control total RNA from BD Biosciences (San Jose, Calif.). All PCR

TABLE 2. Primers for RT-PCR

Primer RT-PCR function	Sequence	Predicted size (bp)
YopM$^-$ mutant construction		
Left flanking DNA		
LFup	ACATTAGAGCTCTGCCTGTCTCCGTTCTTG	1,183
LFdown	TACTATCTGCAGTGTATGGCCGCAGAGT	
Right flanking DNA		
RFup	TGCTGCAGACGCAAGAGCGTTCAT	1,242
RFdown	ATCTCTCGAGACGCCACCGTTGATTA	
Cytokine message analysis		
IFN-γ Forward	5′ TAC TGC CAC GGC ACA GTC ATT GAA 3′	406
IFN-γ Reverse	5′ GCA GCG ACT CCT TTT CCG CTT CCT 3′	
TNF-α Forward	5′ ATG AGC ACA GAA AGC ATG ATC 3′	276
TNF-α Reverse	5′ TAC AGG CTT GTC ACT CGA ATT 3′	
IL-1β Forward	5′ CAG GAT GAG GAC ATG AGC ACC 3′	447
IL-1β Reverse	5′ CTC TGC AGA CTC AAA CTC CAC 3′	
IL-4 Forward	5′ ACG GAG ATG GAT GTG CCA AAC GTC 3′	279
IL-4 Reverse	5′ CGA GTA ATC CAT TTG CAT GAT GC 3′	
IL-6 Forward	5′ GAA AAT CTG CTC TGG TCT TCT GG 3′	227
IL-6 Reverse	5′ TTT TCT GAC CAC AGT GAG GAA TG 3′	
IL-10 Forward	5′ CTG CTC CAC TGC CTT GCT CTT ATT 3′	275
IL-10 Reverse	5′ GTG AAG ACT TTC TTT CAA ACA AAG 3′	
IL-12 Forward	5′ GGA GAC CCT GCC CAT TGA ACT 3′	407
IL-12 Reverse	5′ CAA CGT TGC ATC CTA GCA TCG 3′	
IL-15 Forward	5′ GAA TAC ATC CAT CTC GTG CTA CT 3′	422
IL-15 Reverse	5′ TTT GCA AAA ACT CTG TGA AGG 3′	
IL-15Rα Forward	5′ TGC TGC TGC TGC TGT TGC TA 3′	386
IL-15Rα Reverse	5′ TGT CTC TGT GGT CAT TGC GGT AT 3′	
IL-18 Forward	5′ GCC TCT AGA GTG AAC ATT ACA GAT TTA TCC CCA 3′	436
IL-18 Reverse	5′ ACC GAA TTC ACT GTA CAA CCG CAG TAA TAG GGA 3′	
β-Actin Forward	5′ GTG GGC CGC TCT AGG CAC CA 3′	245
β-Actin Reverse	5′ CGC TTG GCC TTA GGG TTC AGG GGG G 3′	

products were examined on 2% (wt/vol) agarose gels stained with ethidium bromide.

RESULTS

Contribution of YopM to *Y. pestis* growth in vivo. Previous studies have reported that YopM is required for systemic plague infection (14). To gain information on the types of host defenses targeted by YopM, initial experiments determined when during infection the absence of YopM affected bacterial growth and the character of the overall host response in the reticuloendothelial organs where *Y. pestis* growth begins after intravenous infection. We gave 100 CFU of *Y. pestis* KIM5 or the *yopM* deletion mutant *Y. pestis* KIM5-3002 (YopM$^-$) intravenously to B6 mice to mimic septicemic plague. This dose was above the LD_{50} of the parent strain and below the LD_{50} of the mutant (Table 1 and unpublished data). The mice were killed humanely over a period of 10 days postinfection.

During the first 4 days of infection, the KIM5 parental strain and the YopM$^-$ strain displayed similar growth kinetics in spleen and liver; however, tissues infected by the KIM5 strain contained higher bacterial numbers (Fig. 1, open symbols, panels A and B). This difference was statistically significant by *t* test (at $P < 0.05$) starting on day 2 postinfection. After day 4 postinfection, the numbers of YopM$^-$ bacteria began to decrease in both the spleen and liver, dropping to an undetectable level by day 10. In contrast, the KIM5 bacteria continued to increase in viable numbers in both spleen and liver through day 5 postinfection, and the mice succumbed by day 5 or 6. These experiments provided the first clues that YopM may function early in infection, as it is needed for maximal bacterial growth during the initial 4 days of infection. However, at the fourth day postinfection, a major threshold is crossed, where if YopM is absent, the yersiniae are cleared from organs.

As with bacterial growth, the histopathology early in infection by the two *Y. pestis* strains was similar but at day 4 postinfection became dramatically different. On day 2 postinfection, livers and spleens of mice infected with either the KIM5 parent strain or the YopM$^-$ mutant displayed similar localized foci of acute inflammation, containing polymorphonuclear neutrophils (PMNs) and macrophages (Fig. 2). However, at day 4

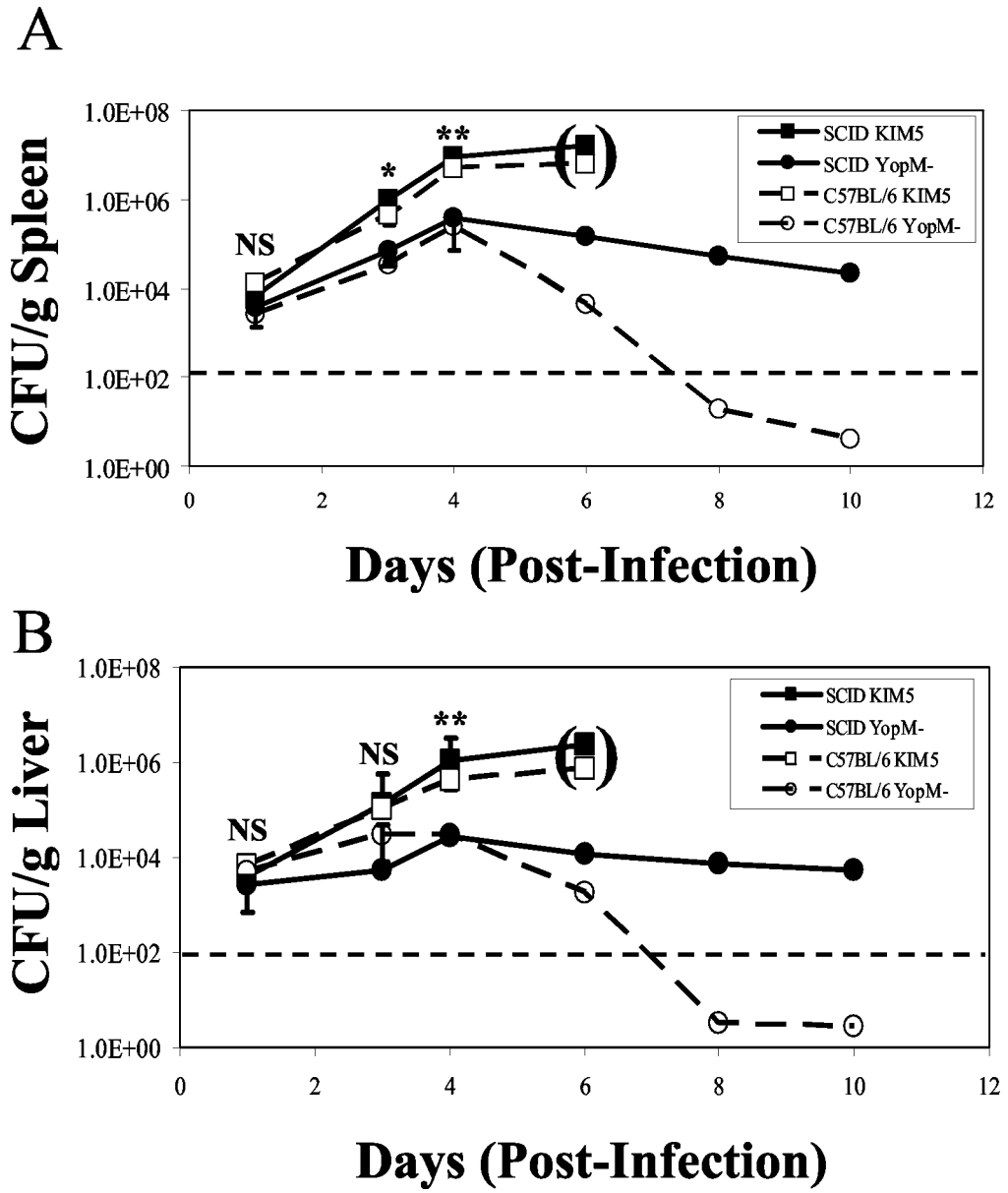

FIG. 1. Time course of infection with *Y. pestis* KIM5 and the YopM$^-$ mutant in B6 and SCID mice. B6 mice (open symbols) and SCID mice (solid symbols) were infected with 100 CFU of *Y. pestis* KIM5 (squares) or *Y. pestis* KIM5-3002 (YopM$^-$, circles). On days 1, 3, 4, 6, 8, and 10, three mice from each group were killed, and CFU were determined on spleens (A) and livers (B). The horizontal dotted lines indicate the lowest numbers of CFU per organ detected with at least 30 CFU per plate. The mice infected with the parent strain KIM5 were all morbid by day 5 and had died several hours prior to preparation for CFU analysis (indicated by the parentheses). Data are averages plus standard deviations and are representative of three independent experiments. *t* tests were performed to measure statistical significance (NS, not significantly different; *, significantly different at $P < 0.05$; **, significantly different at $P < 0.01$).

postinfection, the foci in livers and spleens from mice infected with parent *Y. pestis* KIM5 had evolved into large areas of bland necrosis, as described previously (21, 41, 45) (Fig. 3A), which in the spleen nearly decimated the white pulp regions (Fig. 3C). In contrast, livers from mice infected with the YopM$^-$ mutant displayed numerous granuloma-like lesions at day 4 postinfection (Fig. 3B), and the white pulp of the spleen remained morphologically intact (Fig. 3D). Thus, it appeared that YopM not only promoted better growth in infected animals but also contributed to the development of widespread necrosis in the liver and spleen.

Contribution of innate and adaptive immune responses to growth of the parent KIM5 and YopM$^-$ strains of *Y. pestis*. The finding that YopM has a significant influence on events early in infection of normal mice suggested that YopM may counteract innate defenses. To test this idea, infections with the KIM5 parent and YopM$^-$ mutant also were performed in lymphocyte-deficient SCID mice (B6 background). If YopM affects

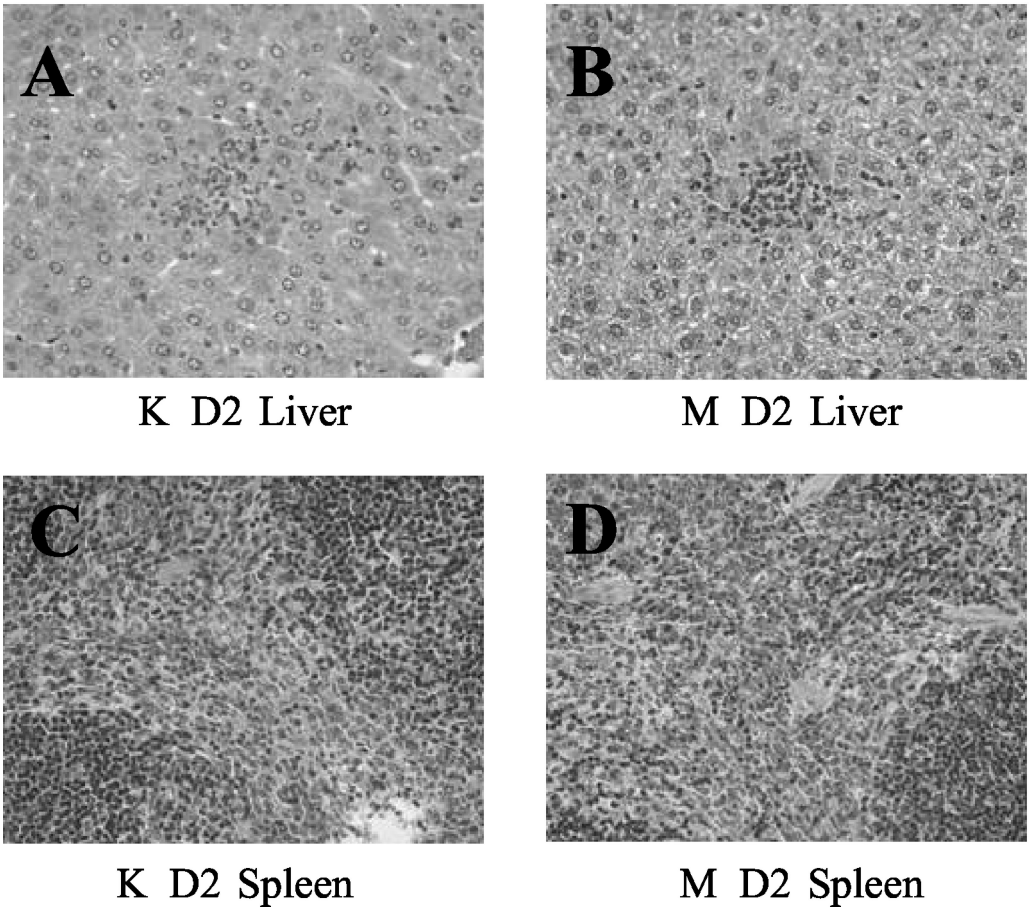

FIG. 2. Histopathology 2 days after infection of mice with the parent *Y. pestis* KIM5 or the YopM$^-$ mutant strain. Mice that were infected simultaneously with the mice in Fig. 1 with *Y. pestis* KIM5 (K) or the YopM$^-$ mutant (M) were processed at intervals thereafter for histological examination. Findings on day 2 postinfection are illustrated. *Y. pestis* KIM5-infected liver (A) and spleen (C); YopM$^-$ mutant-infected liver (B) and spleen (D).

the innate immune response, then the early time course of changes in histopathology and viable bacterial numbers in SCID mice should be similar to that observed in B6 mice. However, if adaptive immunity is targeted by YopM, then the infection kinetics would likely be considerably different in SCID mice. A dose of 100 CFU of either KIM5 or YopM$^-$ yersiniae was given to groups of SCID mice alongside the B6 mice described earlier, and the infection process was followed both quantitatively by plate counts and qualitatively by histopathology over a 10-day period. The KIM5 strain behaved similarly in the SCID and B6 mice, reaching levels of 10^7 CFU/g in spleen and 10^6 CFU/g in liver by day 5 postinfection, when the animals succumbed to the infection (Fig. 1). The histopathology of *Y. pestis* KIM5 infection in SCID mice also was similar to that seen in B6 mice (Fig. 3E), with bland necrotic lesions evident by day 4 postinfection in spleen and liver.

In SCID mice infected with the YopM$^-$ bacteria, the time courses for growth and histopathology over the first 4 days of infection were similar to those for similarly infected B6 mice (Fig. 1, 3F, and 3B). However, beyond day 4, bacterial counts remained elevated in the livers of SCID mice and declined slowly in the spleen, but the yersiniae were cleared in B6 mice by day 10. These data demonstrate clearly that YopM is necessary for lethality in SCID mice and that YopM may counteract innate immunity. The data also indicate that the adaptive immune response is required for efficient elimination of the YopM$^-$ strain beyond day 4 of infection and that expression of YopM in the KIM5 strain may inhibit the ability of the adaptive immune response to clear *Y. pestis*.

NK cells are depleted by infection with *Y. pestis* KIM5. To determine how YopM expression enhances the growth potential of *Y. pestis* during the innate immune response, a flow cytometric analysis of immune cells in several tissues was performed over the course of systemic plague infection. B6 mice were infected with 100 CFU of *Y. pestis* KIM5 or theYopM$^-$ mutant, and immune cell populations in the spleen, liver, and blood were enumerated by flow cytometry. Similar changes in B cells, PMNs, and macrophages were seen in the liver and spleen during infection with either *Y. pestis* strain (Table 3). T-cell numbers gradually declined for both infection groups, with larger decreases being seen during infection with the parent *Y. pestis* later in infection, particularly for CD8$^+$ T cells (Table 3). In contrast, NK cells were depleted dramatically in both spleen (Fig. 4) and liver (data not shown) in mice infected with *Y. pestis* KIM5, but not in mice infected with the YopM$^-$

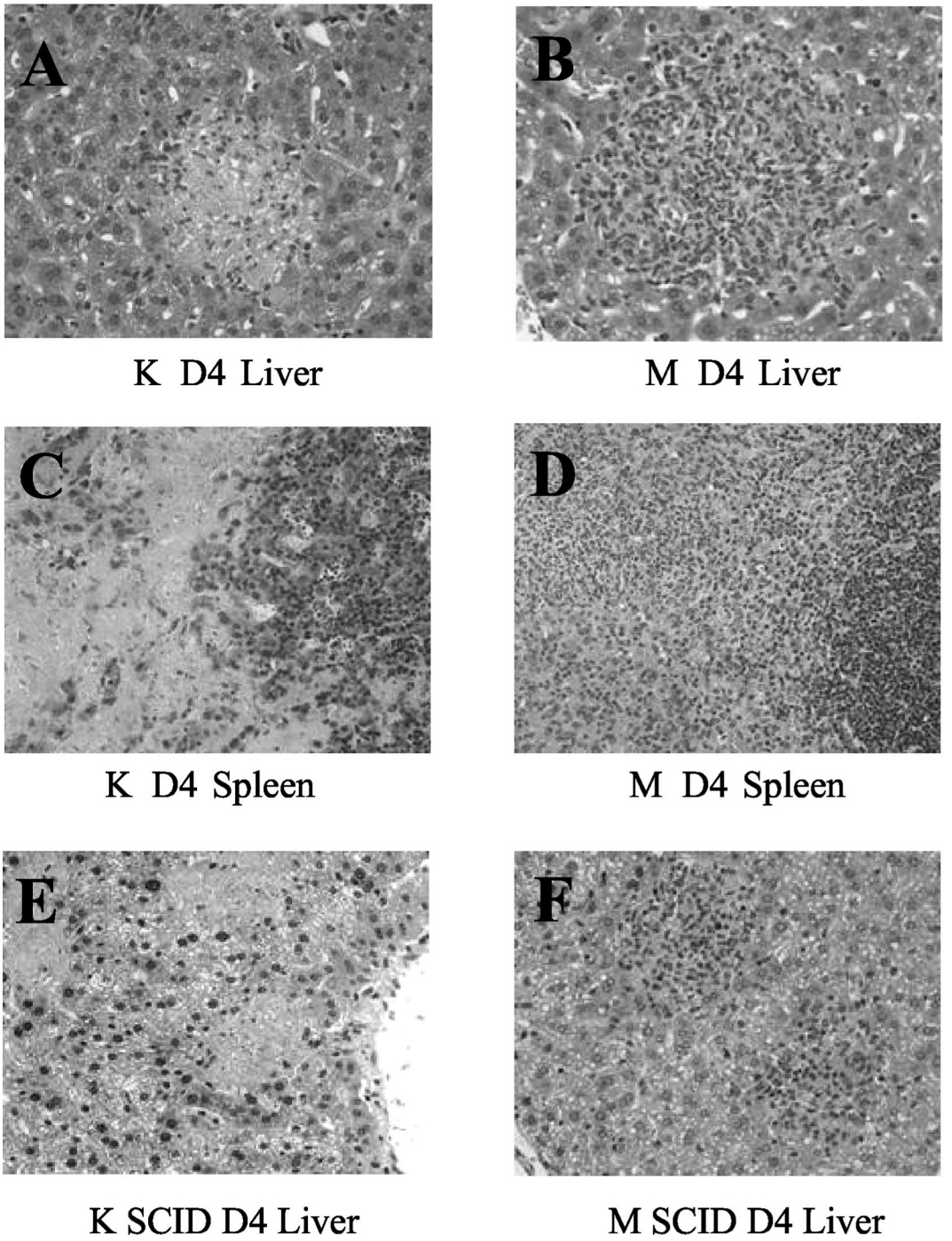

FIG. 3. Histopathology on day 4 postinfection in B6 and SCID mice infected with KIM5 (K) or YopM$^-$ (M) *Y. pestis*. Mice infected simultaneously with those in the experiment in Fig. 1 were processed for histopathological examination on day 4 postinfection Panels A, B, C, and D, B6 mice. Panels E and F, SCID mice. (A and E) Liver, *Y. pestis* KIM5. (B and F) Liver, YopM$^-$ mutant. (C) Spleen, *Y. pestis* KIM5. (D) Spleen, YopM$^-$ mutant.

mutant. The magnitude of this depletion did vary from experiment to experiment, but it was always greater than 20-fold by day 5 postinfection This effect was not simply due to loss of the NK1.1 marker, because similar results were obtained when NK cells were stained for the pan-NK marker CD49b (data not shown).

The spleens from the two groups of mice did progressively differ in weight during infection, with spleens infected with the parent *Y. pestis* being about 10% smaller than those in uninfected mice by day 4 postinfection and those infected with the YopM$^-$ mutant being two- to threefold larger. However, this difference was mostly due to engorgement by red blood cells in

TABLE 3. Average populations of $CD4^+$ and $CD8^+$ T cells, $CD19^+$ B cells, $GR1^+$ PMNs, and $F4/80^+$ macrophages taken from infected spleen samples during infection

Cells and infecting strain	Total no. of cells per spleen (10^6)[a]					
	Day 1	Day 2	Day 3	Day 4	Day 5	Day 8
$CD4^+$ T cells						
KIM5	20.4 ± 3.1	13.2 ± 0.7	10.3 ± 0.6	8.5 ± 3.1	**9.3 ± 1.3**	NA
$YopM^-$	17.7 ± 3.9	16.4 ± 3.8	11.2 ± 1.0	12.9 ± 2.3	14.6 ± 2.4	10.5 ± 1.4
Noninfected	15.9 ± 2.5					
$CD8^+$ T cells						
KIM5	9.4 ± 3.2	6.5 ± 0.3	**4.7 ± 0.5**	**5.4 ± 0.1**	**4.3 ± 1.5**	NA
$YopM^-$	10.6 ± 1.4	7.8 ± 1.5	**6.4 ± 1.0**	**9.6 ± 2.3**	**10.2 ± 1.2**	10.8 ± 1.2
Noninfected	9.8 ± 1.2					
$CD19^+$ B cells						
KIM5	12.4 ± 2.4	21.2 ± 1.0	22.2 ± 1.7	17.0 ± 4.4	19.1 ± 3.3	NA
$YopM^-$	16.1 ± 4.0	18.5 ± 1.0	23.8 ± 1.2	19.3 ± 3.0	18.3 ± 4.3	15.9 ± 1.7
Noninfected	14.6 ± 1.8					
$GR1^+$ PMNs						
KIM5	7.9 ± 3.8	9.4 ± 0.1	7.7 ± 0.2	7.4 ± 1.0	7.9 ± 1.0	NA
$YopM^-$	5.4 ± 0.4	10.0 ± 0.4	11.6 ± 1.6	11.9 ± 3.6	10.2 ± 3.0	8.8 ± 1.0
Noninfected	7.1 ± 1.4					
$F4/80^+$ macrophages						
KIM5	11.9 ± 4.6	11.6 ± 0.4	11.1 ± 3.0	15.2 ± 4.7	14.3 ± 1.6	NA
$YopM^-$	14.1 ± 4.7	15.0 ± 7.1	12.3 ± 2.9	16.9 ± 4.4	19.1 ± 3.4	16.3 ± 4.0
Noninfected	12.6 ± 1.5					

[a] Values are the number of $CD45^+$ splenocytes expressing the indicated surface marker (analysis was performed on $CD45^+$ cells gated by forward and side scatter properties as described in Materials and Methods) and the standard deviation determined from the three samples analyzed for each group. Values that differed significantly between the KIM5 and $YopM^-$ groups are in bold. NA, not available.

the spleens of mice infected with the mutant, as the total numbers of splenocytes from the two groups of mice were similar after lysis of red cells. Moreover, spleen sizes and cell numbers varied similarly in mice infected by the $YopM^-$ mutant and a $YopH^-$ mutant, where NK cell numbers decreased like those in mice infected by the parent *Y. pestis* (see below). Accordingly, differences in NK cells seen between the mice infected with the parent versus $YopM^-$ mutant *Y. pestis* were not due to changes in total numbers of splenocytes.

To determine whether NK cell depletion occurred systemically or was due to an inability of NK cells to extravasate into tissues, NK cell populations in blood were also evaluated. Inability to leave blood would be expected to cause NK cell numbers to be maintained in blood or even increase. Instead, the percentage of $NK1.1^+$ lymphocytes was reduced fivefold at 5 day postinfection in mice infected with *Y. pestis* KIM5, while NK cell numbers were unchanged in mice infected with the $YopM^-$ mutant (Fig. 5), suggesting that *Y. pestis* was causing a systemic reduction in NK cells during infection. Nonetheless, both strains of *Yersinia* stimulated an influx of inflammatory cells into blood: there was a fivefold increase in the populations of PMNs over the first 3 days of infection (Table 4). PMN numbers continued to rise as the bacteria continued to grow in mice infected with the parent *Y. pestis* but gradually subsided in mice infected with the $YopM^-$ mutant as the yersiniae were cleared. B cells and monocytes did not significantly differ in numbers in blood from the two groups of mice, but T-cell populations did decline later in infection, with greater changes occurring in the parent *Y. pestis*-infected mice. Accordingly, the presence of YopM correlated with systemic declines in the numbers of both NK cells and T cells, with the important distinction that with NK cells (Fig. 4), the decreased numbers in blood accompanied much larger depletions in liver and spleen.

NK cell depletion still occurs in *Y. pestis* unable to express a different Yop. The findings above prompted the question of whether the loss of any essential Yop might render the yersiniae unable to alter the nutritional environment of the infectious focus sufficiently for another virulence property such as LcrV to cause decreased numbers of NK cells during infection. To address this issue, B6 mice were infected with *Y. pestis* KIM5-3003, lacking expression of another Yop, YopH, that also is crucial for virulence. The infection dose was modified for this experiment, because the $YopH^-$ mutant was more avirulent than the $YopM^-$ *Y. pestis* (Table 1). When mice were infected with the usual 10^2 yersiniae, the $YopH^-$ mutant failed to grow beyond 5×10^3 per g of spleen and elicited only a minor early inflammatory response (data not shown). To have a meaningful comparison, the $YopH^-$ and $YopM^-$ mutants needed to be present in similar numbers in organs. Accordingly, we used higher doses of the mutants that were approximately 10-fold below their respective LD_{50} doses (Fig. 6).

Although the $YopH^-$ mutant initially was present in larger numbers, it was initially cleared more rapidly than was the $YopM^-$ strain; but the bacterial numbers in spleen (Fig. 6A) and liver (data not shown) were similar for the two mutants during days 2 through 4 postinfection. However, the mice infected with the $YopH^-$ mutant showed the same depression of NK cell numbers that was seen in mice infected with the parent *Y. pestis*, whereas NK cell numbers were higher in mice in-

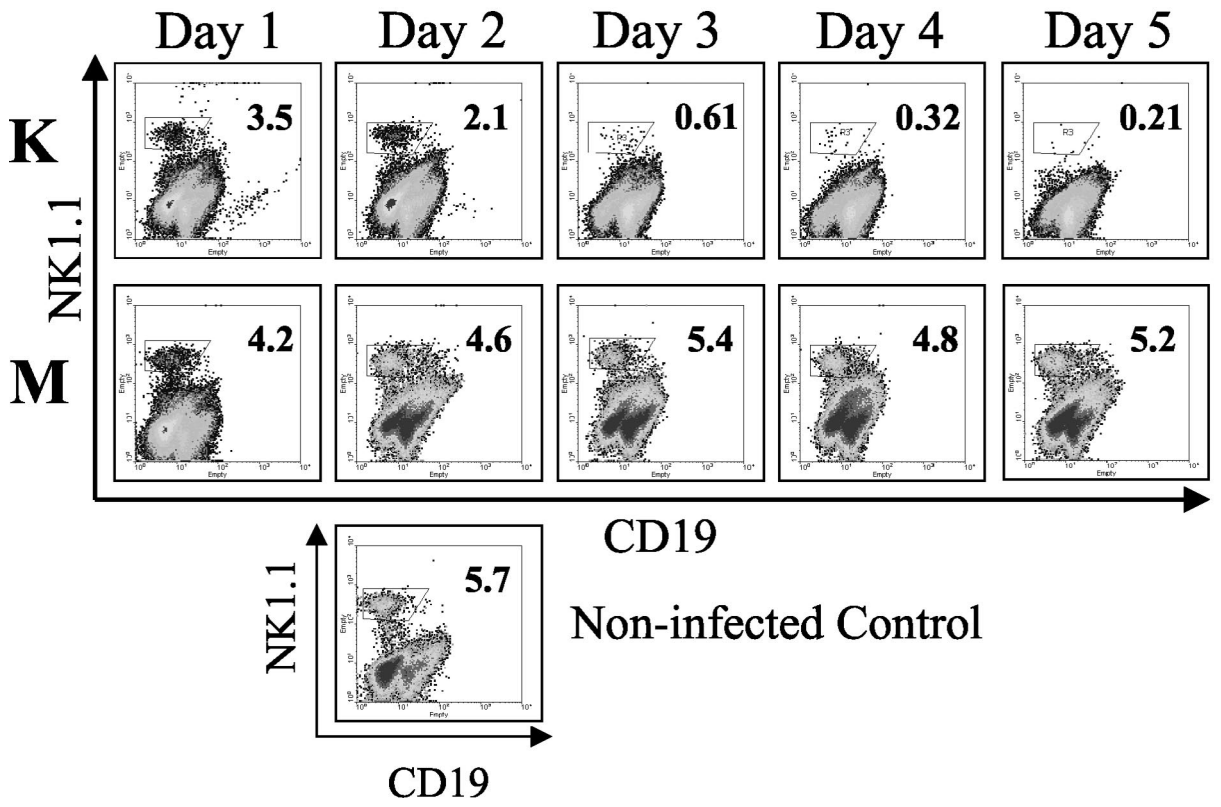

FIG. 4. Flow cytometric analysis of NK cells from spleens of B6 mice infected with *Y. pestis* KIM5 (K) or the YopM$^-$ mutant (M) *Y. pestis* strain. Spleens were obtained from groups of three mice 1 through 5 days after infection. Flow cytometric analysis of myeloid cells from a representative mouse is shown. Numbers in the upper right for each panel give the percentage of myeloid cells that stained strongly for the NK1.1 surface marker. Single panel, noninfected mouse. The data are from one of four similar experiments.

fected with the YopM$^-$ mutant (Fig. 6B). At day 5 postinfection, when the YopH$^-$ yersiniae had been mostly cleared, the numbers of NK cells were beginning to recover. These data show that the failure to cause a depletion in NK cell numbers was not a general effect due to loss of any Yop but instead was specifically due to the loss of YopM in the infecting *Y. pestis* strain.

Expression of key cytokines in mice infected with the parent *Y. pestis* KIM5 and the YopM$^-$ mutant. To explore the basis for the loss of NK cells and the concomitant inability of infected mice to control numbers of the parent *Y. pestis* during infection, the expression of mRNA for IL-1β, IL-4, IL-6, IL-10, IL-12, IL-18, TNF-α, and IFN-γ was compared in mice infected with the KIM5 or YopM$^-$ *Y. pestis* strain. Sometimes by day 2 postinfection but always by day 4 postinfection, basal or reduced net levels of cytokines were observed in mice infected with *Y. pestis* KIM5 (Fig. 7A), with the greatest effect seen for IL-12 and IL-18 in spleen and little effect seen for IL-6 (not illustrated). The small amounts of mRNAs for these cytokines did not correlate with any increase in either IL-10 or IL-4 mRNA. In contrast, mRNA levels were elevated in spleens and livers infected with the YopM$^-$ mutant at both day 2 and day 4 postinfection.

To determine whether the changes in cytokine message levels in tissues reflected those in NK cells and macrophages, these cell types were purified from infected spleens and livers and evaluated for net abundance of mRNA for IFN-γ (in NK cells) and IL-1β, IL-4, IL-6, IL-10, IL-12, IL-18, and TNF-α (in macrophages). In macrophages, a detectable increase in cytokine mRNA was observed by day 2 of infection, compared to noninfected controls, with the exception of IL-4 and IL-10 (Fig. 7B). (The very low IL-18 expression at day 2 in Fig. 7B was not seen in other experiments.) The message levels then declined by day 4 postinfection in macrophages isolated from animals infected with the KIM5 parent strain, but not in cells from mice infected with the YopM$^-$ mutant (Fig. 7B; data for liver not shown).

A similar pattern was seen for IFN-γ message in NK cells (Fig. 7C). Interestingly, in two of three experiments, IFN-γ message declined in NK cells from mice infected with the parent *Y. pestis* as early as day 2 postinfection (Fig. 7C), indicating that YopM is modulating immune function early in infection. Note that although NK cell numbers were declining in mice infected with the parent *Y. pestis*, this experiment analyzed equal numbers of purified NK cells from mice infected with the two *Y. pestis* strains. Accordingly, the NK cells that were present in the spleens of the parent *Y. pestis*-infected mice were not activated. Because the same relative expression of the cytokines was seen for whole tissue and the isolated cells, this indicates that macrophages and NK cells were important sources for the observed changes. Thus, the systemic loss of NK cells when YopM was present in the infecting *Y. pestis* strain correlated with a reduction in the ability of macrophages and NK cells to produce inflammatory cytokines.

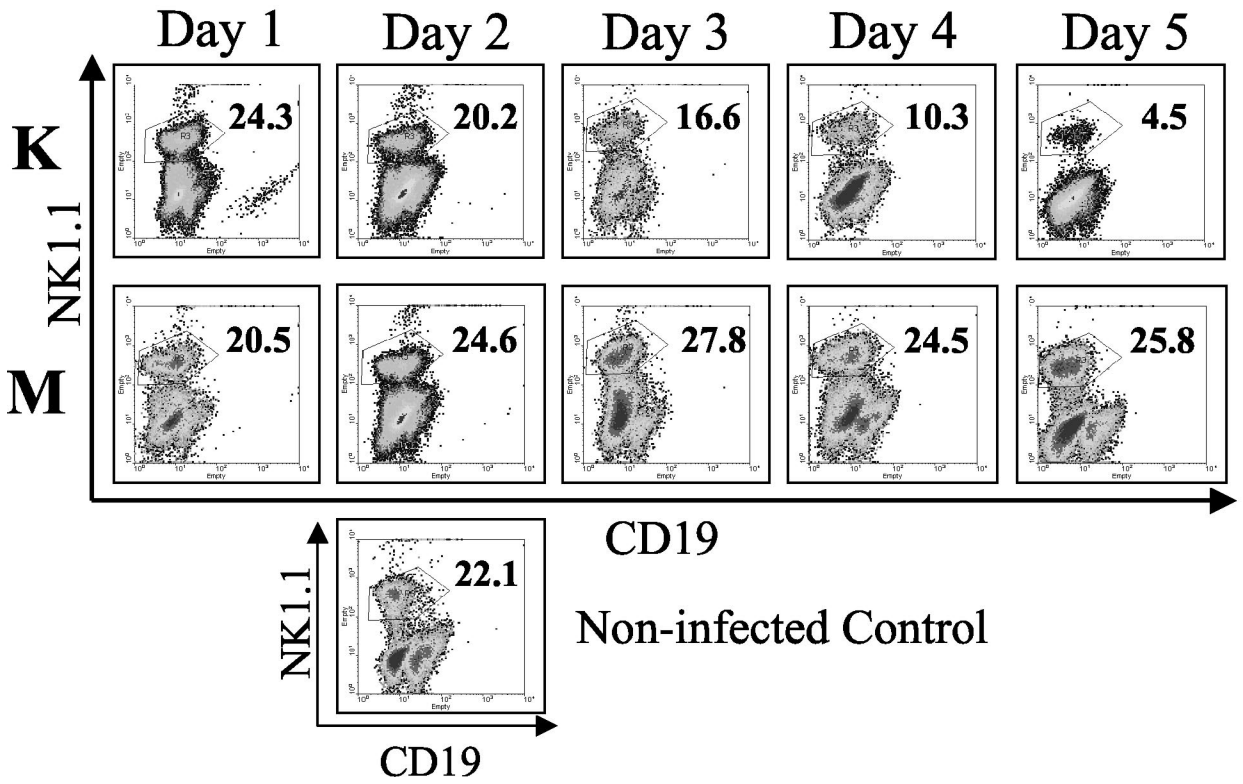

FIG. 5. Flow cytometric analysis of NK cells from the blood of individual B6 mice infected with parent *Y. pestis* KIM5 (K) or the YopM$^-$ (M) strain. Cells from groups of three mice per bacterial strain per time point were collected from whole blood on Lympholyte gradients on days 1, 2, 3, 4, and 5 postinfection. Flow cytometric analysis was done as outlined for Fig. 4. Single panel, noninfected mouse. The data are from one of three similar experiments.

Expression of IL-15 and IL-15 receptor in mice infected with *Y. pestis* KIM5 and the YopM$^-$ mutant. Previous studies have indicated that IL-15 is crucial for both the maintenance of viability in circulating NK cells and the ability of NK cells to become activated and produce IFN-γ upon stimulation (12, 30, 31, 46). Because a global depletion of NK cells occurred in the *Y. pestis* KIM5-infected mice and not the mice infected with the YopM$^-$ mutant, experiments were initiated to determine if YopM may be affecting the levels of IL-15 or its specific receptor alpha chain (IL-15Rα) during the course of infection. Analysis of net message abundance for IL-15 in whole spleen tissue showed a decrease in both the *Y. pestis* KIM5-infected and YopM$^-$ mutant-infected mice at day 4 postinfection (Fig. 8A). However, analysis of purified macrophages demonstrated low IL-15 mRNA levels in cells isolated from mice infected with *Y. pestis* KIM5 at day 4, while the level of expression was elevated in the mice infected with the YopM$^-$ mutant (Fig. 8B). Surprisingly, there was little or no mRNA for the IL-15Rα chain in NK cells isolated from mice infected with the parent *Y. pestis* strain KIM5 on day 2, and the level remained low on day 4, while there were increased amounts in NK cells isolated on both days from mice infected with the YopM$^-$ *Y. pestis* (Fig. 8C). NK cells appeared to be especially susceptible to loss of IL-15 receptor message expression, because purified macrophages from mice infected with the parent *Y. pestis* did not display reduced expression until day 4 (data not shown).

DISCUSSION

Previous studies in BALB/c mice have shown that YopM$^-$ *Y. pestis* is reduced in virulence by four orders of magnitude compared to *Y. pestis* KIM5, but the mechanism that accounts for this reduced virulence remained unclear. The present study revealed that *Y. pestis* caused a global depletion of NK cells and a loss of activation by both NK cells and macrophages. These effects depended on the presence of YopM in the infecting yersiniae and were manifested by day 2 after infection by significantly higher numbers of viable bacteria for the parent *Y. pestis* than the YopM$^-$ mutant in infected tissues, suggesting an effect of YopM on the innate immune response. To test this hypothesis, SCID mice were infected with the parent *Y. pestis* and the YopM$^-$ mutant to determine if the absence of YopM still affected virulence in the absence of B and T cells. Bacterial growth in SCID mice mirrored that in normal mice, with bacterial numbers always being lower for the YopM$^-$ mutant. This finding supported the hypothesis that YopM may negatively affect the early innate immune response and thereby promote the growth of *Y. pestis* in vivo. Importantly, both SCID and B6 mice survived infection with the YopM$^-$ mutant, whereas both mouse strains succumbed to infection by the parent *Y. pestis*. These results showed that YopM was required for lethality in SCID mice that lacked an adaptive immune

TABLE 4. Average populations of $CD4^+$ and $CD8^+$ T cells, $CD19^+$ B cells, $GR1^+$ PMNs, and $F4/80^+$ monocytes taken from infected blood samples during infection

Cells and infecting strain	Total no. of cells per ml of blood (10^5)[a]					
	Day 1	Day 2	Day 3	Day 4	Day 5	Day 8
$CD4^+$ T cells						
KIM5	4.0 ± 0.9	4.6 ± 1.1	**1.7 ± 0.9**	**1.1 ± 0.4**	**1.1 ± 0.3**	NA
$YopM^-$	5.1 ± 1.7	6.8 ± 1.4	**4.9 ± 0.6**	**4.6 ± 0.5**	**3.9 ± 0.3**	5.8 ± 0.4
Noninfected	10.0 ± 1.9					
$CD8^+$ T cells						
KIM5	3.2 ± 0.4	2.5 ± 0.4	**1.8 ± 0.1**	**1.0 ± 0.2**	**0.8 ± 0.1**	NA
$YopM^-$	4.2 ± 0.7	3.1 ± 0.5	**2.4 ± 0.6**	**2.7 ± 0.4**	**3.1 ± 0.8**	5.4 ± 0.9
Noninfected	4.2 ± 0.3					
$CD19^+$ B cells						
KIM5	6.2 ± 0.8	5.3 ± 0.1	3.6 ± 0.1	3.3 ± 0.2	3.8 ± 0.3	NA
$YopM^-$	6.6 ± 0.7	6.0 ± 1.3	4.7 ± 1.0	6.5 ± 0.6	4.7 ± 0.8	5.5 ± 0.7
Noninfected	9.5 ± 0.9					
$GR1^+$ PMNs						
KIM5	3.2 ± 1.1	14.3 ± 2.7	16.2 ± 3.2	19.8 ± 2.4	24.5 ± 1.3	NA
$YopM^-$	3.8 ± 0.5	15.8 ± 2.3	18.8 ± 3.2	18.8 ± 2.2	11.8 ± 1.9	10.3 ± 2.3
Noninfected	3.5 ± 0.3					
$F4/80^+$ monocytes						
KIM5	6.3 ± 0.7	6.8 ± 4.4	10.7 ± 1.1	8.8 ± 1.2	6.6 ± 0.6	NA
$YopM^-$	5.8 ± 0.5	9.5 ± 2.4	13.0 ± 3.2	14.0 ± 3.4	11.5 ± 4.5	7.5 ± 3.0
Noninfected	6.9 ± 1.6					

[a] Values are number of $CD45^+$ blood leukocytes expressing the indicated surface marker (analysis was performed on $CD45^+$ cells gated by forward and side scatter properties as described in Materials and Methods) and standard deviation determined from three samples analyzed for each group. Values that differed significantly between the KIM5 and $YopM^-$ groups are in bold. NA, not available.

response. Hence, YopM's virulence mechanism targeted the innate component of the immune response.

To determine which component of the innate immune system was targeted by YopM, changes in the populations of immune cell types were analyzed by flow cytometry in mice infected by either the parent or $YopM^-$ *Y. pestis* strain. A similar acute inflammatory response occurred during the first 3 days of infection by parent and mutant *Y. pestis*, as indicated by similar increases in Grl^+ PMNs and $F4/80^+$ macrophages in the spleen and liver; thereafter, the inflammatory response tracked the growth of the parent *Y. pestis* and clearance of the $YopM^-$ mutant. However, the percentage of $NK1.1^+$ (or $CD49a^+$) NK cells was dramatically reduced in spleens and livers only from mice infected with *Y. pestis* KIM5. This indicated that YopM targets the innate immune system at the level of NK cells, causing their rapid elimination during infection. Analysis of the percentage of NK cells in blood indicated that YopM caused a systemic loss of NK cells rather than a change in the ability of NK cells to leave the blood.

Although YopM's primary target may lie in the innate immune system, an effective adaptive immune response was required to eliminate the $YopM^-$ yersiniae from infected tissues, as SCID mice retained large numbers of bacteria during the observation period. These studies did not indicate whether YopM had an effect on the induction or effector phase of the adaptive immune response, since all mice succumbed to infection by the parent *Y. pestis* strain regardless of the presence of functional adaptive immunity. Future investigation will be required to assess the significance of the severalfold decline in numbers of both $CD4^+$ and $CD8^+$ T cells during infection, seen more strongly when YopM was present in the infecting strain.

In addition to a decrease in NK cell numbers, there was drastically reduced expression of IFN-γ message by the NK cells that remained in the spleen and liver of mice infected with the parent *Y. pestis*, and this was seen as early as day 2 postinfection. Numerous reports have indicated that the production of IFN-γ by NK cells is necessary for early activation of macrophages to mediate robust bactericidal activity and strong expression of Th1 cytokines (13, 43). Moreover, both NK cells and macrophages can produce the Th1 cytokines IL-12 and IL-18 as well as TNF-α during bacterial infections. When the expression of message for inflammatory cytokines was analyzed from infected animals, those for Th1 cytokines IL-12 and IL-18 and for TNF-α were all found to be lower at day 4 in mice infected with *Y. pestis* KIM5 than in mice infected with the $YopM^-$ mutant.

Isolated macrophages also showed decreased levels of mRNA for these cytokines as well as the proinflammatory cytokine IL-1β, while the amounts of IL-6 message were not significantly affected (Fig. 7 and data not shown). This decrease appeared not to be due to increased message for either IL-10 or IL-4, which have been shown to inhibit development of the Th1 immune response (5, 6, 26); however, this study did not rule out possible changes in these cytokines at the translational and posttranslational levels. Concomitant with diminished cytokine mRNA expression in macrophages, both whole tissue and isolated NK cells showed drastically reduced levels of mRNA for IFN-γ. The decreased number of NK cells and poor NK cell activation may have been responsible for de-

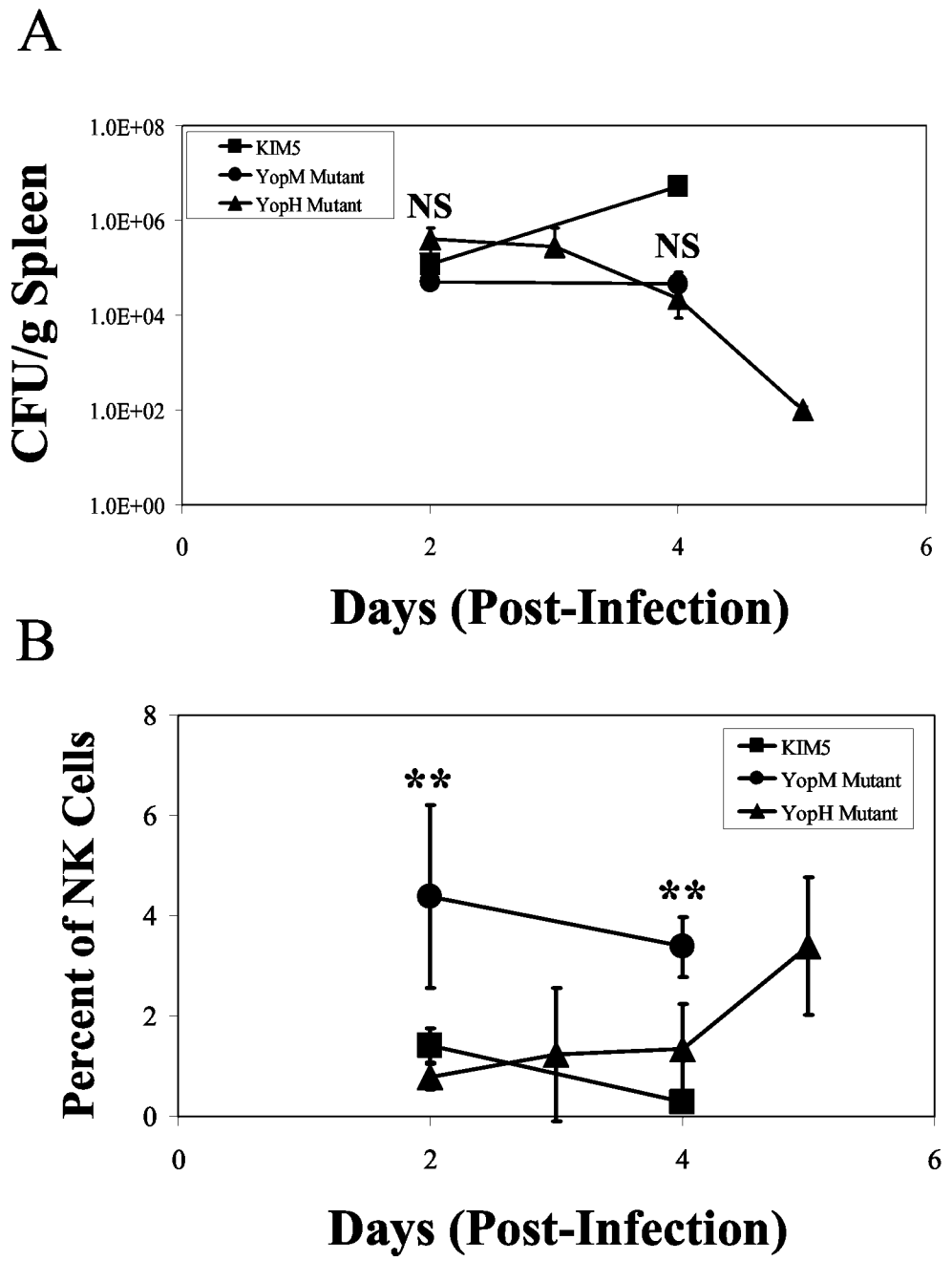

FIG. 6. Comparisons of bacterial CFU and NK cell numbers in spleens after infection of B6 mice with the YopH$^-$ mutant or YopM$^-$ mutant or the parent strain of *Y. pestis*. B6 mice were infected with 4×10^6 cells of the YopH$^-$ mutant *Y. pestis* KIM5-3003 (triangles) or 6×10^3 cells of the YopM$^-$ mutant (circles) or 10^2 cells of the parent *Y. pestis* KIM5 (squares). At the indicated times postinfection, the numbers of CFU (A) and NK cells (B) were determined in spleens. The data represent the average ± standard deviation for three mice per datum point and are from one of two similar experiments. *t* tests were performed to measure statistical significance (NS, not significantly different; **, significantly different at $P < 0.01$).

creased production of inflammatory cytokines by macrophages and decreased macrophage effector function.

The loss of IFN-γ expression in the *Y. pestis* KIM5-infected mice may have contributed to the histopathology in the livers and spleens of these animals. A large body of evidence documents the importance of IFN-γ production in the formation of granulomas (1, 2, 8, 11, 19, 35, 39). With the loss of IFN-γ expression in the mice infected with the parent *Y. pestis*, macrophage activation and granuloma formation were prevented. This could possibly allow more bacterial growth, a more intense acute inflammatory response, and subsequent tissue necrosis, as discussed by others (20). In the present study, the mice infected with the YopM$^-$ mutant continued to express high levels of IFN-γ, which may have promoted activation of

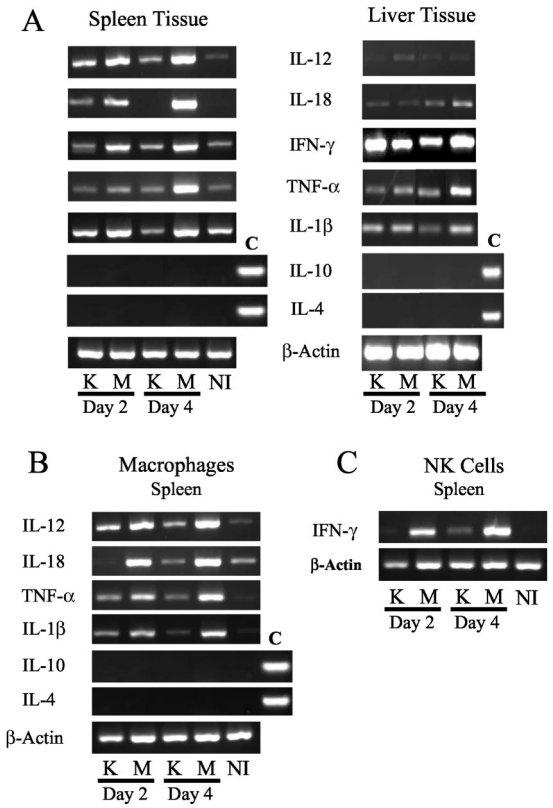

FIG. 7. Reverse transcription-PCR analysis of either whole tissue or cells collected with magnetic beads from spleens and livers of B6 mice infected with KIM5 (K) or YopM$^-$ (M) *Y. pestis*. (A) mRNA was taken from nonfractionated spleen or liver tissue and analyzed for number of proinflammatory cytokines, with β-actin serving as a loading control. (B) mRNA levels from macrophages were analyzed. (C) mRNA from NK cells was examined for the expression of IFN-γ and β-actin. For IL-10 and IL-4 in panels A and B, positive controls are denoted with a C. NI indicates that the data are from noninfected mice. All mRNA samples were normalized by concentration, and equal amounts of cDNA product were loaded in each lane. Data are from one of three similar experiments.

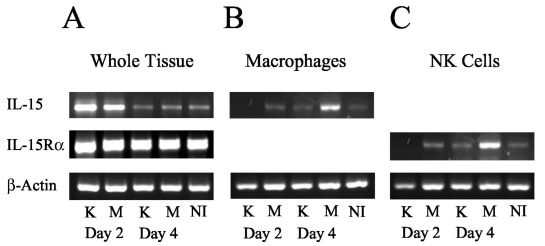

FIG. 8. Reverse transcription-PCR analysis of IL-15 and IL-15Rα mRNA from spleens or splenic cells of B6 mice infected with KIM5 (K) or YopM$^-$ (M) *Y. pestis*. Whole spleen tissue or spleen cells obtained with the use of magnetic beads in the experiments illustrated in Fig. 7 were analyzed for net abundance of mRNA for IL-15 and IL-15Rα. (A) mRNA from whole spleen tissue. (B) mRNA from isolated macrophages. (C) mRNA from isolated NK cells. NI designates data from noninfected mice. All mRNA samples were normalized by concentration, and equal amounts of cDNA product were loaded in each lane.

macrophages and better containment of the bacteria in protective granulomas, with reduction of the acute inflammatory response and associated tissue injury.

To investigate a possible link between an effect of YopM on cytokine expression and both the loss and diminished activation status of NK cells, tests were made to determine if message levels for IL-15 were affected during infection by the parent *Y. pestis*. This cytokine is crucial for the maintenance and activation of circulating NK cells as well as for NK cell development in bone marrow (12, 30, 31, 46). Indeed, the level of IL-15 message was low in macrophages isolated from mice infected with the parent *Y. pestis* at day 4 but not in macrophages from mice infected with the YopM$^-$ mutant. More striking still, message for the IL-15Rα chain was lost from NK cells as early as day 2 of infection but was maintained in NK cells from mice infected with the YopM$^-$ mutant. These data suggest that a possible mechanism by which YopM causes the loss of NK cells is by blocking expression of functional IL-15R on NK cells and inhibiting IL-15 expression by macrophages. Interestingly, the levels of IL-15Rα mRNA appeared normal at day 2 postinfection in both whole tissues and macrophages from mice infected with the parent *Y. pestis* KIM5 (Fig. 8 and data not shown), suggesting that decreased expression of IL-15Rα may be limited to NK cells very early during *Y. pestis* infection.

The molecular mechanism by which YopM inhibits expression of either IL-15 or IL-15Rα remains to be determined. It has been shown in vitro that YopM is delivered to host cells through a type III secretion mechanism and is then transported to the nucleus (38). Studies by McDonald et al. (17) showed that YopM forms complexes with specific serine/threonine kinases that may interact with a number of immunological signaling pathways. Thus, it is possible that one of these affected pathways may be involved in the signaling pathway of IL-15 or its receptor. It is also possible that YopM may play a posttranscriptional or posttranslational role in inhibiting the production of either IL-15 or its receptor. Indeed, microarray analysis of bone marrow-derived macrophages infected with *Y. enterocolitica* WA revealed no immediate transcriptional effects (2 h after infection) that could be attributed to YopM (9).

Either way, YopM must be delivered to each affected cell by direct bacterial contact to exert its effect, and this poses the intriguing question of how a bacterial virulence protein delivered locally can have a global effect. It is possible that a diffusible factor from inflammatory or parenchymal cells in the focus of infection mediates YopM's NK cell-specific downregulating effect on IL-15Rα. However, it also is possible that *Y. pestis* directly delivers YopM to NK cells as they enter the inflammatory focus. This would be consistent with the observation of drastically decreased amounts of IL-15Rα mRNA in NK cells at a time when macrophages and tissue as a whole were unaffected for this message and little affected for others. It also would account for the larger extent of the NK cell depletion that was seen in liver and spleen compared to blood. This does not rule out the possibility that yersiniae also deliver Yops to macrophages and PMNs when the bacteria encounter these cells, with important pathogenic effects on Rho family GTPases and signaling through mitogen-activated protein kinases and NF-κB. Macrophages and PMNs have not been ruled out as target cells for YopM. Indeed, macrophages from mice infected with parent (but not YopM$^-$) *Y. pestis* showed

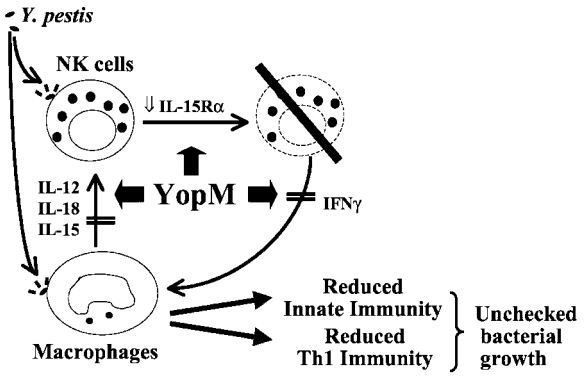

FIG. 9. Model for the pathogenic role of YopM in plague. Both macrophages and NK cells are hypothesized to be important targets of infection by *Y. pestis*. Delivery of YopM into macrophages promotes a decrease in the expression of IL-12, IL-18, and IL-15. YopM delivery into NK cells inhibits expression of IL-15Rα, which promotes systemic depletion of NK cells. The depletion of NK cells limits the early production of IFN-γ during infection, which affects innate immunity by decreasing the capacity of macrophages to become activated early during infection. A reduced ability to generate an effective Th1 adaptive immune response occurs due to reduced expression of IL-12 and IL-18. The result is unchecked growth of yersiniae during both the innate and adaptive phases of the immune response.

downregulated message levels for key Th1 cytokines, possibly indicating the action of an inhibitory process, as opposed to merely failure to increase levels beyond those achieved early in infection. Future work will need to determine which cells actually receive Yops from *Y. pestis* in vivo and to sort out which effects are direct consequences of YopM action and which are indirect.

One scenario that fits the data obtained so far is that both macrophages and NK cells are targets of YopM (Fig. 9), causing decreased production of IL-15 by macrophages and reduced responsiveness to IL-13 by NK cells. This would prevent activation of NK cells at the focus of infection and initiate a pathway that leads to NK cell death. Indeed, in two of three experiments, there was a significant decrease in abundance of mRNA for IFN-γ in NK cells as early as day 2 of infection. As a result, macrophages fail to be fully activated, and bacterial growth is unchecked. Delivery of YopM into macrophages as well as into NK cells may diminish the ability of the innate immune response to direct the development of a Th1 adaptive immune response, preventing effective clearance of the pathogen.

It is becoming clear that yersiniae have multiple mechanisms for suppression of the mammalian innate immune response. LcrV can elicit IL-10 production by monocyte/macrophages, with resulting downregulated expression of TNF-α and IFN-γ; YopJ causes downregulation of NF-κB and mitogen-activated protein kinase pathways and also causes downregulated production of proinflammatory cytokines, including TNF-α; and this study has shown that YopM also inhibits the innate immune response. The findings have revealed that YopM mediates a novel pathogenic effect that represents a new class of virulence mechanism, because the global depletion of NK cells has not been demonstrated previously in any infectious process. Future investigation will determine how the multiple immune-suppressing effects are integrated during plague: it is possible that they are not truly redundant and have roles during different phases of infection.

ACKNOWLEDGMENTS

This research was supported by PHS (NIAID) grant AI41668. During part of this study, EJK was supported by the Training Program in Microbial Pathogenesis (PHS [NIAID] T32-AI-49795).

We gratefully acknowledge Ela Skrzypek for creation of the YopM$^-$ mutant, Christine Wulff-Strobel and Martin Ward for creation of the YopH$^-$ mutant, and Clarissa Cowan and Sandra Burnett for assistance in some of the experiments.

REFERENCES

1. **Bean, A. G. D., D. R. Roach, H. Briscoe, M. P. France, H. Korner, J. D. Sedgwick, and W. J. Britton.** 1999. Structural deficiencies in granuloma formation in TNF gene-targeted mice underlie the heightened susceptibility to aerosol *Mycobacterium tuberculosis* infection, which is not compensated for by lymphototoxin. J. Immunol. **162:**3504–3511.
2. **Chiu, B., C. M. Freeman, V. R. Stolberg, E. Komuniecki, P. M. Lincoln, S. L. Kunkel, and S. W. Chensue.** 2003. Cytokine-chemokine networks in experimental Mycobacterial and Schistosomal pulmonary granuloma formation. Am. J. Resp. Cell Mol. Biol. **29:**106–116.
3. **Cornelis, G. R.** 1998. The *Yersinia* deadly kiss. J. Bacteriol. **180:**5495–5504.
4. **Cornelis, G. R.** 2002. *Yersinia* type III secretion: send in the effectors. J. Cell Biol. **158:**401–408.
5. **Fiorentino, D. F., A. Zlotnik, T. R. Mosmann, M. Howard, and A. O'Garra.** 1991. IL-10 inhibits cytokine production by activated macrophages. J. Immunol. **147:**3815–3822.
6. **Fiorentino, D. F., A. Zlotnik, P. Viera, T. R. Mosmann, M. Howard, K. W. Moore, and A. O'Garra.** 1991. IL-10 acts on the antigen-presenting cell to inhibit cytokine production by Th1 cells. J. Immunol. **146:**3444–3451.
7. **Galyov, E. E., S. Hakansson, Å. Forsberg, and H. Wolf-Watz.** 1993. A secreted protein kinase of *Yersinia pseudotuberculosis* is an indispensable virulence determinant. Nature **361:**730–732.
8. **Hein, J., V. A. J. Kempf, J. Diebold, N. Bucheler, S. Preger, I. Horak, A. Sing, U. Kramer, and I. Autenrieth.** 2000. Interferon consensus sequence binding protein confers resistance against *Yersinia enterocolitica*. Infect. Immun. **68:**1408–1417.
9. **Hoffmann, R. K. vanErp, K. Trülzsch, and J. Heesemann.** 2004. Transcriptional responses of murine macrophages to infection with *Yersinia enterocolitica*. Cell. Microbiol. **6:**377–390.
10. **Holmström, A. J. Olsson, P. Cherepanov, E. Maier, R. Nordfelth, J. Pettersson, R. Benz, H. Wolf-Watz, and Å. Forsberg.** 2001. LcrV is a channel size-determining component of the Yop effector translocon of *Yersinia*. Mol. Microbiol. **39:**620–632.
11. **Jouanguy, E., R. Doffinger, S. Dupuis, A. Pallier, F. Altare, and J. L. Casanova.** 1999. Il-12 and IFN-gamma in host defense against mycobacteria and salmonella in mice and men. Curr. Opin. Immunol. **11:**346–351.
12. **Kennedy, M. K., M. Glaccum, S. N. Brown, E. A. Butz, J. L. Viney, M. Embers, N. Matsuki, K. Charrier, L. Sedger, C. R. Willis, K. Brasel, P. J. Morrissey, K. Stocking, J. C. L. Schuh, S. Joyce, and J. J. Peschon.** 2000. Reversible defects in natural killer and memory CD8 T cell lineages in interleukin 15-deficient mice. J. Exp. Med. **191:**771–780.
13. **Lanier, L. L.** 1997. NK cells—from no receptor to too many. Immunity **6:**371–378.
14. **Leung, K. Y., B. S. Reisner, and S. C. Straley.** 1990. YopM inhibits platelet aggregation and is necessary for virulence of *Yersinia pestis*. Infect. Immun. **58:**3262–3271.
15. **Leung, K. Y., and S. C. Straley.** 1989. The *yopM* gene of *Yersinia pestis* encodes a released protein having homology with the human platelet surface protein GPIbα. J. Bacteriol. **171:**4623–4632.
16. **Marenne, M. N., L. Journet, L. J. Mota, and G. Cornelis.** 2003. Genetic analysis of the formation of the Ysc-Yop translocation pore in macrophages by *Yersinia enterocolitica*: role of LcrV, YscF and YopN. Microb. Pathog. **35:**243–258.
17. **McDonald, C., P. Vacratsis, J. B. Bliska, and J. E. Dixon.** 2003. The *Yersinia* virulence factor YopM forms a novel protein complex with two cellular kinases. J. Biol. Chem. **278:**18514–18523.
18. **Metcalf, W. W., W. Jiang, L. L. Daniels, S. K. Kim, A. Haldimann, and B. L. Wanner.** 1996. Conditionally replicative and conjugative plasmids carrying lacZ alpha for cloning, mutagenesis, and allele replacement in bacteria. Plasmid **35:**1–13.
19. **Mielke, M. E., C. Peters, and H. Hahn.** 1997. Cytokines in the induction and expression of T-cell-mediated granuloma formation and protection in the murine model of listeriosis. Immunol. Rev. **158:**79–93.
20. **Nakajima, R., and R. R. Brubaker.** 1993. Association between virulence of *Yersinia pestis* and suppression of gamma interferon and tumor necrosis factor alpha. Infect. Immun. **61:**23–31.
21. **Nakajima, R. V. L. Motin, and R. R. Brubaker.** 1995. Suppression of cyto-

kines in mice by protein A-V antigen fusion peptide and restoration of synthesis by active immunization. Infect. Immun. **63:**3021–3029.
22. **Nedialkov, Y. A., V. L. Motin, and R. R. Brubaker.** 1997. Resistance to lipopolysaccharide mediated by the *Yersinia pestis* V antigen-polyhistidine fusion peptide: amplification of interleukin-10. Infect. Immun. **65:**1196–1203.
23. **Nilles, M. L., A. W. Williams, E. Skrzypek, and S. C. Straley.** 1997. *Yersinia pestis* LcrV forms a stable complex with LcrG and may have a secretion-related regulatory role in the low-Ca^{2+} response. J. Bacteriol. **179:**1307–1316.
24. **Nilles, M. L., K. A. Fields, and S. C. Straley.** 1998. The V antigen of *Yersinia pestis* regulates Yop vectoral targeting as well as Yop secretion through effects on YopB and LcrV. J. Bacteriol. **180:**3410–3420.
25. **Orth, K., Z. Xu, M. B. Mudgett, Z. Q. Bao, L. E. Palmer, J. B. Bliska, W. F. Mangel, B. Staskawicz, and J. E. Dixon.** 2000. Disruption of signaling by *Yersinia* effector YopJ, a ubiquitin-like protein protease. Science **290:**1594–1597.
26. **Oswald, I. P., R. T. Gazzinelli, A. Sher, and S. L. James.** 1992. IL-10 synergizes with IL-4 and transforming growth factor-β to inhibit macrophage cytotoxic activity. J. Immunol. **148:**3578–3582.
27. **Persson, C., R. Nordfelth, A. Holmström, S. Håkansson, R. Rosqvist, and H. Wolf-Watz.** 1995. Cell-surface bound *Yersinia* translocate the protein tyrosine phosphatase YopH by a polarized mechanism into the target cell. Mol. Microbiol. **18:**135–150.
28. **Petterson, J., A. Holström, J. Hill, S. Leary, E. Frithz-Lindsten, A. von-Euler-Matell, E. Carlsson, R. Titbal, Å. Forsberg, and H. Wolf-Watz.** 1999. The V-antigen of *Yersinia* is surface exposed before target cell contact and involved in virulence protein translocation. Mol. Microbiol. **32:**961–976.
29. **Price, S. B., C. Cowan, R. D. Perry, and S. C. Straley.** 1991. The *Yersinia pestis* V antigen is a regulatory protein necessary for Ca^{2+}-dependent growth and maximal expression of low-Ca^{2+} response virulence genes. J. Bacteriol. **173:**2649–2657.
30. **Prlic, M., B. R. Blazar, M. A. Farrar, and S. C. Jameson.** 2003. In Vivo survival and homeostatic proliferation of natural killer cells. J. Exp. Med. **197:**967–976.
31. **Ranson, T., C. A. J. Vosshenrich, E. Corcuff, O. Richard, W. Muller, and J. P. DiSanto.** 2003. IL-15 is an essential mediator of peripheral NK-cell homeostasis. Blood **101:**4887–4893.
32. **Reed, L. J., and H. Muench.** 1938. A simple method of estimating fifty percent endpoints. Am. J. Hyg. **27:**493–497.
33. **Reisner, B. S., and S. C. Straley.** 1992. *Yersinia pestis* YopM: thrombin binding and overexpression. Infect. Immun. **60:**5242–5252.
34. **Rosqvist, R., K.-E. Magnusson, and H. Wolf-Watz.** 1994. Target cell contact triggers expression and polarized transfer of the *Yersinia* YopE cytotoxin into mammalian cells. EMBO J. **13:**964–972.
35. **Schaible, U. E., H. L. Collins, and S. H. Kaufmann.** 1999. Confrontation between intracellular bacteria and the immune system. Adv. Immunol. **71:**267–377.
36. **Shao, F., P. O. Vacratsis, Z. Bao, K. E. Bowers, C. A. Fierke, and J. E. Dixon.** 2003. Biochemical characterization of the *Yersinia* YopT protease: Cleavage site and recognition elements in Rho GTPases. Proc. Natl. Acad. Sci. USA **100:**904–909.
37. **Sing, A., A. Roggenkamp, A. M. Geiger, and J. Heesemann.** 2002. *Yersinia enterocolitica* evasion of the host immune response by V antigen-induced IL-10 production of macrophages is abrogated in IL-10-deficient mice. J. Immunol. **168:**1315–1321.
38. **Skrzypek, E., C. Cowan, and S. C. Straley.** 1998. Targeting of the *Yersinia pestis* YopM protein into HeLa cells and intracellular trafficking to the nucleus. Mol. Microbiol. **30:**1051–1065.
39. **Souto, J. T., F. Figueiredo, A. Furlanetto, K. Pfeffer, M. A. Rossi, and J. S. Silva.** 2000. Interferon-γ and tumor necrosis factor-α determine resistance to *Paracoccidioides brasiliensis* infection in mice. Am. J. Pathol. **156:**1811–1820.
40. **Straley, S. C., and W. S. Bowmer.** 1986. Virulence genes regulated at the transcriptional level by Ca^{2+} in *Yersinia pestis* include structural genes for outer membrane proteins. Infect. Immun. **51:**445–454.
41. **Straley, S. C., and M. L. Cibull.** 1989. Differential clearance and host-pathogen interactions of $YopE^-$ and $YopK^-$ $YopL^-$ *Yersinia pestis* in BALB/c mice. Infect. Immun. **57:**1200–1210.
42. **Straley, S. C., E. Skrzypek, G. V. Plano, and J. B. Bliska.** 1993. Yops of *Yersinia* spp. pathogenic for humans. Infect. Immun. **61:**3105–3110.
43. **Unanue, E. R.** 1997. Studies in listeriosis show strong symbiosis between the innate cellular system and T-cell response. Immunol. Rev. **158:**11–25.
44. **Une, T., and R. R. Brubaker.** 1984. In vivo comparison of avirulent Vwa^- and Pgm^- or Pst^r phenotypes of yersiniae. Infect. Immun. **43:**895–900.
45. **Une, T., R. Nakajima, and R. R. Brubaker.** 1986. Roles of V antigen in promoting virulence in yersiniae. Contrib. Microbiol. Immunol. **9:**179–185.
46. **Waldmann, T. A., and Y. Tagaya.** 1999. The multifaceted regulation of interleukin-15 expression and the role of this cytokine in NK cell differentiation and host response to intracellular pathogens. Annu. Rev. Immunol. **17:**19–49.
47. **Wulff-Strobel, C. R., A. W. Williams, and S. C. Straley.** 2002. LcrQ and SycH function together at the Ysc type III secretion system in *Yersinia pestis* to impose a hierarchy of secretion. Mol. Microbiol. **43:**411–423.

Editor: D. L. Burns